

Neurovascular coupling preserved in a chronic mouse model of Alzheimer's disease: Methodology is critical

Paul S Sharp^{1,2}, Kamar E Ameen-Ali^{2,3} , Luke Boorman³ ,
Sam Harris^{4,2}, Stephen Wharton⁵, Clare Howarth² ,
Osman Shabir², Peter Redgrave² and Jason Berwick²

Journal of Cerebral Blood Flow & Metabolism
2020, Vol. 40(11) 2289–2303
© The Author(s) 2019



Article reuse guidelines:
sagepub.com/journals-permissions
DOI: 10.1177/0271678X19890830
journals.sagepub.com/home/jcbfm



Abstract

Impaired neurovascular coupling has been suggested as an early pathogenic factor in Alzheimer's disease (AD), which could serve as an early biomarker of cerebral pathology. We have established an anaesthetic regime to allow repeated measurements of neurovascular function over three months in the J20 mouse model of AD (J20-AD) and wild-type (WT) controls. Animals were 9–12 months old at the start of the experiment. Mice were chronically prepared with a cranial window through which 2-Dimensional optical imaging spectroscopy (2D-OIS) was used to generate functional maps of the cerebral blood volume and saturation changes evoked by whisker stimulation and vascular reactivity challenges. Unexpectedly, the hemodynamic responses were largely preserved in the J20-AD group. This result failed to confirm previous investigations using the J20-AD model. However, a final acute electrophysiology and 2D-OIS experiment was performed to measure both neural and hemodynamic responses concurrently. In this experiment, previously reported deficits in neurovascular coupling in the J20-AD model were observed. This suggests that J20-AD mice may be more susceptible to the physiologically stressing conditions of an acute experimental procedure compared to WT animals. These results therefore highlight the importance of experimental procedure when determining the characteristics of animal models of human disease.

Keywords

Barrel cortex, electrophysiology, optical imaging, blood flow, J20

Received: 11 July 2019; Revised 19 September 2019; Accepted 2 November 2019

Introduction

Alzheimer's disease (AD) in humans currently has no effective treatment. Most of our recent insights into the causes of AD are linked to the discovery of increased amounts of beta-amyloid plaques associated with significant neuronal loss.¹ Despite the large investment in both clinical and pre-clinical research resources focussed on the beta-amyloid hypothesis, no effective preventative or remedial treatment has so far been found. Consequently, alternative theories regarding the onset and development of AD have been proposed. One of the notable rival hypotheses is the neurovascular degeneration hypothesis (NDH), first proposed by Zlokovic.^{2,3} It suggests that a functional deficit within cells of the neurovascular unit (neurons, glial cells, pericytes and vascular cells) would deprive active neurons of adequate oxygen and glucose, which could either be the initial trigger of AD, or significantly add to

the disease burden. If correct, the NDH would offer the potential for developing new treatments based on targeting identified dysfunctional cells in the

¹Nanomedicine Lab, Division of Pharmacy and Optometry, School of Health Sciences, Faculty of Biology, Medicine and Health, The University of Manchester, Manchester, UK

²Department of Psychology, University of Sheffield, Sheffield, UK

³Institute of Neuroscience, Newcastle University, Newcastle upon Tyne, UK

⁴UK Dementia Research Institute, UCL Institute of Neurology, University College London, London, UK

⁵Department of Neuroscience, Sheffield Institute for Translational Neuroscience, University of Sheffield, Sheffield, UK

Corresponding author:

Jason Berwick, Department of Psychology, University of Sheffield, Floor D, Cathedral Court, 1 Vicar Lane, Sheffield, South Yorkshire S1 1HD, UK.
Email: j.berwick@sheffield.ac.uk

neurovascular unit. With the aid of modern neuroimaging methods (e.g. functional magnetic resonance imaging – fMRI), measurements of the progressive breakdown of neurovascular coupling (NVC) could also act as an early biomarker of AD. A recent study analysing data from the Alzheimer's disease neuroimaging initiative (ADNI⁴) suggested that cerebrovascular dysfunction may be the earliest pathological event to emerge, possibly marking the beginning of the disease process. This report alone highlights the need for more research into the NDH.

A problem facing investigations of the neurovascular unit is that the technologies currently used with human subjects do not have the spatial and temporal resolution required to understand the basic mechanistic processes involved. To address this issue, transgenic mouse models of AD have been developed and now play a critical role in investigating the underlying mechanisms responsible for the AD-like disease state. A range of models has been produced which partially mimic different aspects of human AD (see reviews^{5,6}). These include the increased A β plaque load, Tau or combinations of both. While transgenic mouse models may not perfectly replicate all aspects of the human condition, the hope is that they share the critical features that will enable the underlying mechanisms to be discovered. Pre-clinical AD mouse models allow the use of more invasive technologies to measure both hemodynamic and neuronal variables in more detail throughout disease development. Consequently, several groups have reported disruptions to NVC in transgenic AD mice that overexpress human amyloid precursor protein (hAPP).^{7–11} These studies used laser Doppler flowmetry (LDF) or Laser speckle imaging to measure cerebral blood flow (CBF) from a restricted cortical region in acutely anaesthetised animals. Using the J20-AD mouse model (used in 3 of the above studies), we have recently confirmed using an aged match sibling co-hort to the animals used in this study that the mice suffer long-term memory deficits and the expected A β plaque deposition in the hippocampus and cortex by nine-months of age¹² (see Figure 1(c)). Wright et al.¹³ have also confirmed similar behavioural and anatomical decline at similar time points.

To extend these investigations, we have developed a chronic mouse preparation that is sufficiently stable to permit repeated measures of neurovascular function across a three-month period when the disease state is present.¹⁴ Consequently, in sedated J20-AD mice and age-matched wild type controls, we used repeated measures two-dimensional optical imaging spectroscopy (2D-OIS) to record neurovascular responses evoked by sensory stimulation and vascular reactivity challenges. A final acute experiment was conducted in which 2D-OIS and multi-channel electrophysiology

were performed simultaneously. Contrary to expectation, our chronic imaging studies found little or no difference in the hemodynamic responses between J20-AD and WT animals across a range of sensory stimulations and gas challenges. However, in the final acute experiment, reduced NVC function similar to that reported in previous investigations^{7–10} was observed. This difference suggests that the J20-AD mice are more susceptible to the physiological stresses incurred by acute experimental procedures compared with WT controls. These results indicate that experimental conditions are critical when characterising mouse models of human disease, and differences in methodology are likely responsible for the variable and sometimes incompatible results frequently seen in mouse pre-clinical neurovascular studies.

Material and methods

Anesthesia and cranial window surgery

All animal procedures were performed in accordance with the guidelines and regulations of the UK Government, Animals (Scientific Procedures) Act 1986, the European directive 2010/63/EU, and approved by the University of Sheffield Ethical review and licensing committee and in compliance with the ARRIVE guidelines for animal research. Two groups of five animals were used: (i) heterozygous transgenic male C57BL/6 mice that overexpress human APP (hAPP) carrying the human Swedish and Indiana familial AD mutations under control of the PDGF β chain promoter (hAPP-J20 line); and (ii) male wild-type controls. All animals were between 9 and 12 months on the date of surgical preparation. Animals were anesthetized with fentanyl-fluanisone (Hypnorm, Vetapharm Ltd), midazolam (Hypnovel, Roche Ltd) and sterile water (1:1:2 by volume; 7.0 ml/kg, i.p.) for surgery, while anaesthesia during the imaging experiments was further maintained with isoflurane (0.5–0.8%) in 100% oxygen. A homeothermic blanket (Harvard Apparatus) maintained rectal temperature at 37°C. Mice were placed in a stereotaxic frame (Kopf Instruments) and a dental drill was used to thin the skull overlying the right somatosensory cortex to translucency thereby forming an optical window (~4 mm²). A thin layer of clear cyanoacrylate cement was applied to reinforce and smooth the window. This reduced specular reflections during imaging and prevented skull regrowth during the three-month experimental period. A stainless steel imaging chamber was secured over the thinned cranial window using dental cement. This chamber was used to stabilise the head during imaging sessions. After surgery, animals were left to recover for a minimum of seven days before

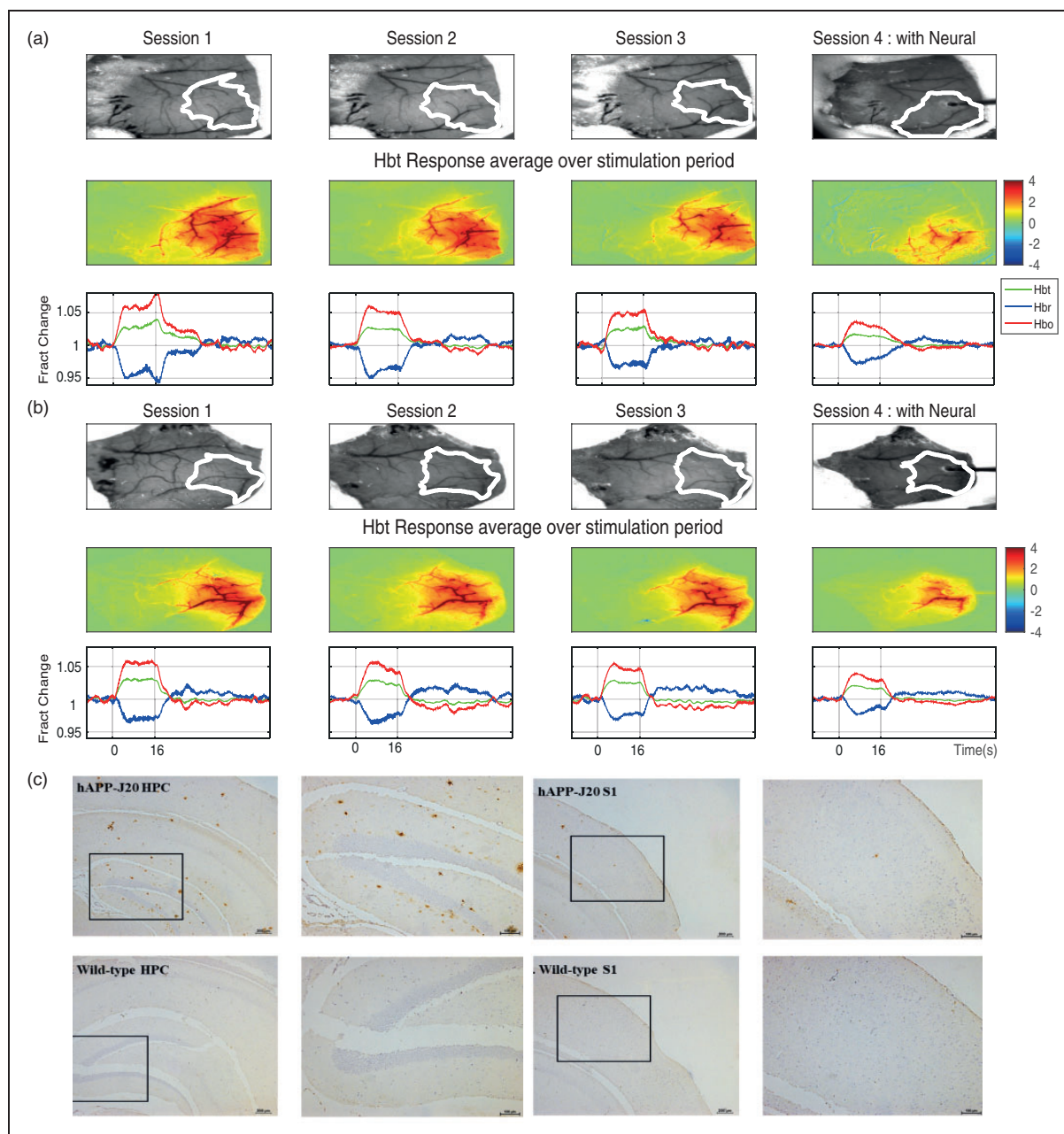


Figure 1. Representative hemodynamic responses from WT (a) and J20-AD mice (b) across three chronic imaging sessions (1–3) each separated by ~30 days and a final acute session (4) where a multi-channel electrode is inserted into the activated whisker region. Activation maps represent the change in Hbt with respect to baseline during a 16-s mechanical whisker stimulation. Time series take for Hbt, Hbr and Hbo are taken from the activated whisker region highlighted in white on the reference images (rows 1 and 3). Hbt: total blood volume, Hbr: oxyhemoglobin, Hbo: deoxyhemoglobin. (c) Representative images of A β plaques from 12-month wild type and J20-AD mice from hippocampus (HPC) and primary somatosensory cortex (S1). There is strong deposition of plaques in the hippocampus but relatively few in the cortex. Top row shows J20-AD mice bottom row WT controls. Column one shows HPC (scale bar = 200 μ m), column two zoomed in box inset regions of HPC (scale bar = 100 μ m), column three S1 cortex with column four showing zoomed in box inset regions of S1.

chronic experimental imaging sessions commenced. During this period, animals were monitored regularly and weighed to ensure they did not fall below 90% of surgical day body weight. Randomisation and blinding were not performed in this study.

Experimental design

All animals were imaged using an anaesthetised condition adapted from our previous published methodology.¹⁴ All animals underwent four imaging sessions.

The first session occurred 7–10 days after cranial window surgery. The following three sessions were each separated by ~30 days. In the last session, a 16-channel electrode was placed in the active whisker barrel region (see below for method of localisation) to provide a measure of concurrent hemodynamic and neural activity. Each session began with an induction of anaesthesia (see methods) followed after 1 h by 2D-OIS. In the last acute (4th) imaging session, imaging started 30 min after the electrode had been inserted. Each 2D-OIS session comprised eight separate experiments performed in a set order. Each experiment separated from the previous one by ~3 min during which time we acquired a dark image used to remove camera noise from the spectroscopy data.

Exp1: Short duration sensory stimulation breathing 100% oxygen: With the animal breathing oxygen (100%), there were 30 successive trials of 25 s; 5 s after the start of each trial, whisker stimulation was administered for 2 s. Together, 750 s of continuous data was collected. For all stimulation experiments, the whiskers contralateral to the imaging chamber were mechanically deflected using a plastic T-bar attached to a stepper motor under computer control. Whiskers were deflected ~1 cm in the rostral-caudal direction at 5 Hz.

Exp2: Exp1 was repeated to ensure preparation and recording stability.

Exp3: Mild gas challenge: while the animal transitioned from breathing oxygen to normal air. 2D-OIS lasted 750 s with the transition to air occurring after 105 s.

Exp4: Short duration sensory stimulation breathing air: Used the same paradigm as Exp1 except the animal was breathing normal air rather than 100% oxygen.

Exp5: Long duration sensory stimulation breathing air: 15 × 70 s consecutive trials with 16-s whisker stimulation (5 Hz) presented after 10 s. Total record comprised 1050 s of data.

Exp6: Mild gas challenge: while the animal transitioned from breathing air back to 100% oxygen; 750 s of data were recorded with the transition occurring after 105 s.

Exp7: Long duration sensory stimulation under 100% oxygen: 15 × 70 s consecutive trials, with 16 s whisker stimulation at 5 Hz occurring after 10 s. Total record comprised 1050 s of data.

Exp8: Major gas challenge in the form of hypercapnia: 250 s after starting the record, the animal was switched from breathing 100% oxygen to 90% and 10% carbon dioxide. The duration of this challenge was 250 s, after which a further 250 s of data were collected giving a total of 750 s of recorded data.

Statistical analysis

The first question we addressed was whether the evoked haemodynamic responses changed over time

(sessions 1–3) and were different between the J20-AD and WT groups. Separate two-way repeated measures ANOVA's were performed for Hbt, Hbo and Hbr for each of the five whisker stimulation experiments (Exp1,2,4,5,7). A single measure, the mean response size from the stimulation period was calculated and used for the analysis. Based on the results of this analysis (see below), a second repeated measures ANOVA was performed. In this analysis, we averaged the three chronic imaging sessions together to create a single chronic session for both WT and J20-AD mice with the repeated measurement now being stimulation experiment (Exp1,2,4,5,7). This same analysis was also performed for the acute imaging session. This would show if there were any differences between the WT and J20-AD animals in the chronic or acute parts of the study.

2D-OIS

2D-OIS was used to estimate changes in cortical oxyhemoglobin (Hbo), deoxyhemoglobin (Hbr) and total hemoglobin concentration (Hbt). To generate spatial maps of hemodynamic responses, the cortex was illuminated with four wavelengths of light (495 nm, 559 nm, 575 nm and 587 nm) using a Lambda DG-4 high-speed galvanometer (Sutter Instrument Company, USA). Remitted light was collected using a Dalsa 1M60 CCD camera at 184 × 184 pixels (resolution ~75 μm), with a frame rate of the 32 Hz, and synchronised to filter switching, giving an effective frame rate of 8 Hz.

The analysis approach combined the absorption spectra of Hbo and Hbr with Monte-Carlo simulations of photons passing through homogeneous tissue to estimate the mean path-length of photons for each wavelength. Images were then analysed on a pixel-by-pixel basis using a modified Beer–Lambert law, which used the generated mean photon path lengths, to convert the detected attenuation for each wavelength into predicted absorption. The absorption values were then used to generate 2D spatiotemporal image-series of the estimates of the changes in Hbt, Hbo and Hbr from baseline values. All experiments started with the animal breathing 100% oxygen, and for this condition we assumed a concentration of hemoglobin in tissue at 100 μM and saturation set at 70%. We then used the gas transition experiment 3 to assess how these baselines changed when the animal breathed normal air. This was calculated on an individual animal basis. The baseline blood volume and saturation values in air were consistent for both WT and J20-AD mice (Hbt concentration WT = 99.3 ± 0.42 sem, AD = 99.7 ± 0.47 sem; Saturation WT = 62.6% ± 0.6, AD = 62.6 ± 0.6). All hemodynamic

changes were taken as the fractional changes from these baseline estimations.

Selection of regions of interest for 2D-OIS data

In each imaging session, we used the 16 s Hbt data from Exp7 to select the whisker region of interest. During the stimulation period, all pixels that were 1.5 standard deviations above the pre-stimulus baseline were deemed above threshold and a region was drawn around all these activated pixels (see Figure 1). Arteries and veins were identified within the activated region using principal component analyses applied to the Hbt and Hbr images, respectively (see Figure 7).

Multi-channel electrophysiology

For the final acute imaging session, a 16-channel microelectrode (100 μm spacing, site area 177 μm^2 , 1.5–2.7 M Ω impedance; Neuronexus Technologies, Ann Arbor, MI, USA) implanted into the right barrel cortex. The microelectrode was positioned to a depth of 1500 μm in the centre of the activated whisker region defined previously by 2D-OIS. The electrode was connected to a preamplifier and data acquisition device (Medusa BioAmp/RZ5, TDT, Alachua, FL, USA). Neural data were sampled at 6 kHz and recorded continuously throughout each of the eight experiments described above.

Results

Chronic imaging: Sensory stimulation experiments 1,2,4,5 and 7

The thinned cranial window preparation remained stable throughout the three-month's duration of the study with evoked hemodynamic responses remaining remarkably consistent throughout this period for both J20-AD and WT animals (see Figure 1). The first questions we addressed were whether the evoked haemodynamic responses changed over time (sessions 1–3) and were different between the J20-AD and WT groups. Separate two-way repeated measures ANOVA's were performed for Hbt, Hbo and Hbr for each of the five whisker stimulation experiments (Exp1,2,4,5,7, results shown in Supplementary Table 1). For most experiments, there was no effect of group (WT or J20-AD), there was only one result that approached significance. For Hbr in Exp5, there was a difference in the sessions ($F=5.178$ and $p=0.03$) However, after Bonferroni correction (level needed to be less than $p=0.003$), this result was non-significant. Several results did show an effect of session that approached significance in which Session 1 was generally larger than sessions 2

and 3 (Hbt- Exp1,7, Hbo – Exp1, 2,7 and Hbr Exp1,2,4) but all were below the threshold for significance after Bonferroni correction apart from Hbo in Exp7. Thus, in most cases differences between the relevant variables failed to reach acceptable levels of statistical reliability ($p > 0.003$, see Supplementary Table 1). The surprising and remarkable extent to which the haemodynamic responses J20-AD were preserved is illustrated in Figure 2. The stability of response magnitudes across experimental conditions between WT and J20 mice is also summarised in Supplementary Table 2. Because no reliable differences were found in the results between chronic sessions, we averaged haemodynamic time series across chronic to create sessions for a second analysis to test for differences in the haemodynamic responses within experiments (Exp1,2,4,5 and 7) between the WT and J20-AD groups. For each of the hemodynamic measures (Hbt, Hbr, and Hbo), a two-way repeated measure ANOVA was conducted which compared responses evoked by the different stimulation conditions and mouse-type (J20-AD vs. WT). In each of the analyses, the experiment factor was significant (Hbt: $F=16.1$, $p=6.32^{10^{-8}}$; Hbr: $F=5.34$, $p=0.002$; Hbo: $F=13.4$, $p=5.2^{10^{-7}}$), which was to be expected as the stimulations were of varying durations (2s and 16s). On the other hand, no reliable statistical differences were found between the two mouse-types for (Hbt: $F=0.14$, $p=0.71$, Hbr: $F=3.39$, $p=0.07$, Hbo: $F=1.25$, $p=0.26$). In each case, the interactions between experimental condition and mouse-type were also non-significant (Hbt: $F=0.03$, $p=0.99$; Hbr: $F=0.27$, $p=0.89$; Hbo: $F=0.13$, $p=0.97$). Although the experiments within a session were always run in the same order, this time-related confound within these analyses do not obscure the point that the neurovascular performance of J20-AD and WT controls was, for the most part, similar. Specifically, using our chronic procedures, we failed to find the large differences reported in previous studies.

Stimulation experiments 1,2,4,5 and 7 – Acute imaging sessions

The 4th and final session involved acute surgical procedures in which a multi-channel recording electrode was implanted prior to the barrel region being imaged. The concurrent acute recording of electrophysiological and hemodynamic variables in this session produced results that were markedly different from previous chronic imaging sessions (see Figures 3 and 4). First, both WT and J20-AD fractional time series responses were reduced compared to the chronic session data. However, the responses of J20-AD mice were suppressed compared with the corresponding WT responses, especially for experiment 1 (see Figures 3 and 4 and

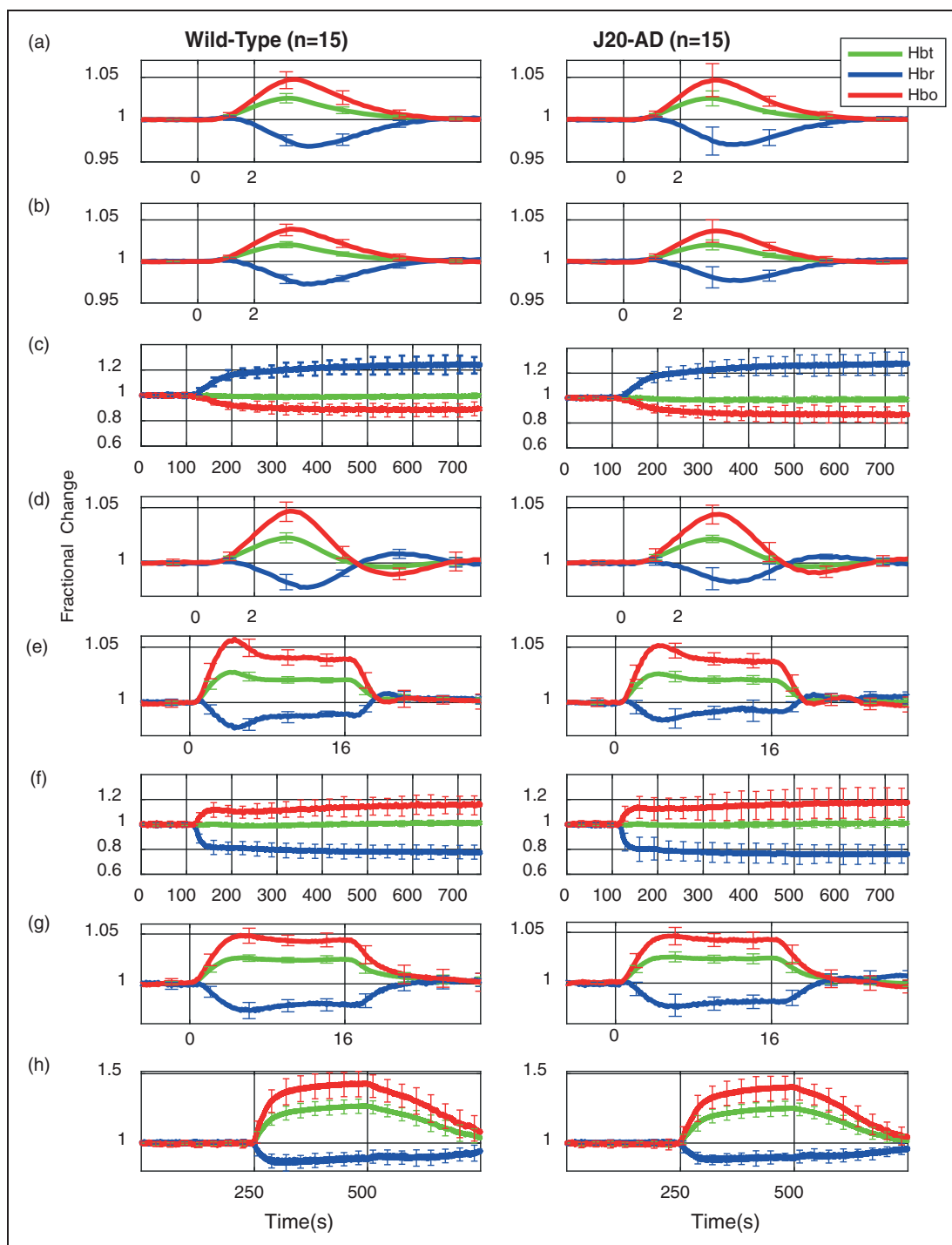


Figure 2. Neurovascular coupling preserved in J20-AD mice. Hemodynamic time series (Hbt, Hbr and Hbo) averaged across chronic sessions for each of the eight experiments (a–h). WT responses are illustrated in the left column and J20-AD in the right column. Error bars = standard deviation.

Supplementary Table 2 for overall values). When the same repeated measures ANOVA analyses for Hbt, Hbo and Hbr were performed on data from the acute imaging session in all conditions, there was now a significant effect of group (Hbt: $F = 13.096$, $p = 0.0008$, Hbr:

$F = 20.45$, $p = 5.34 \times 10^{-7}$, Hbo: $F = 19.08$, $p = 8.6334 \times 10^{-5}$) with all WT responses being larger than J20-AD. The expected experimental session difference was also present (Hbt: $F = 17.43$, $p = 2.35 \times 10^{-7}$, Hbr: $F = 20.45$, $p = 0.004$ Hbo: $F = 16.665$, $p = 4.11 \times 10^{-8}$) but with no significant

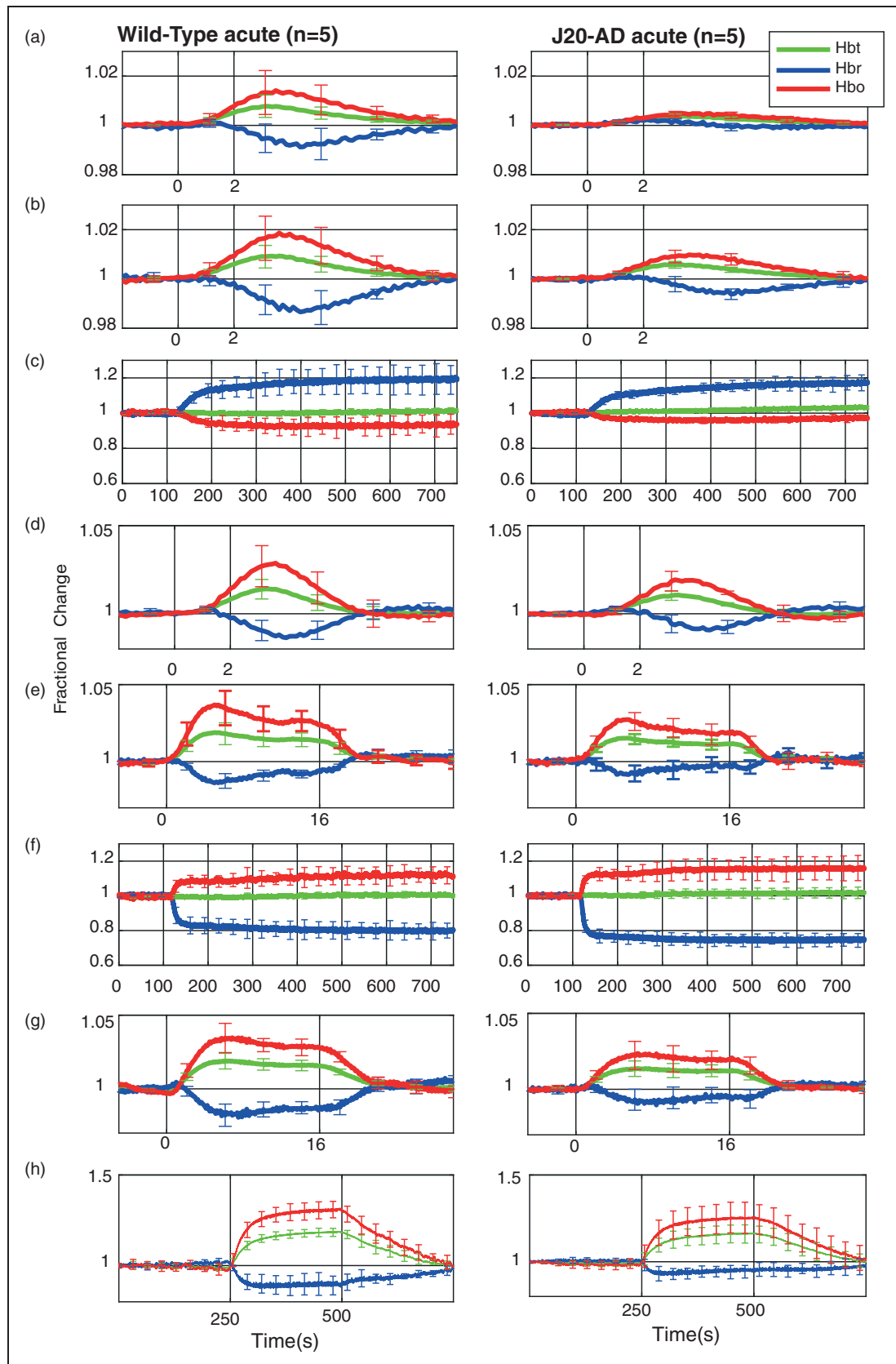


Figure 3. Average hemodynamic time series responses take across all eight experiments (a–h) in for the acute imaging session with WT in the left column and J20-AD in the right column. Error bars =standard deviation.

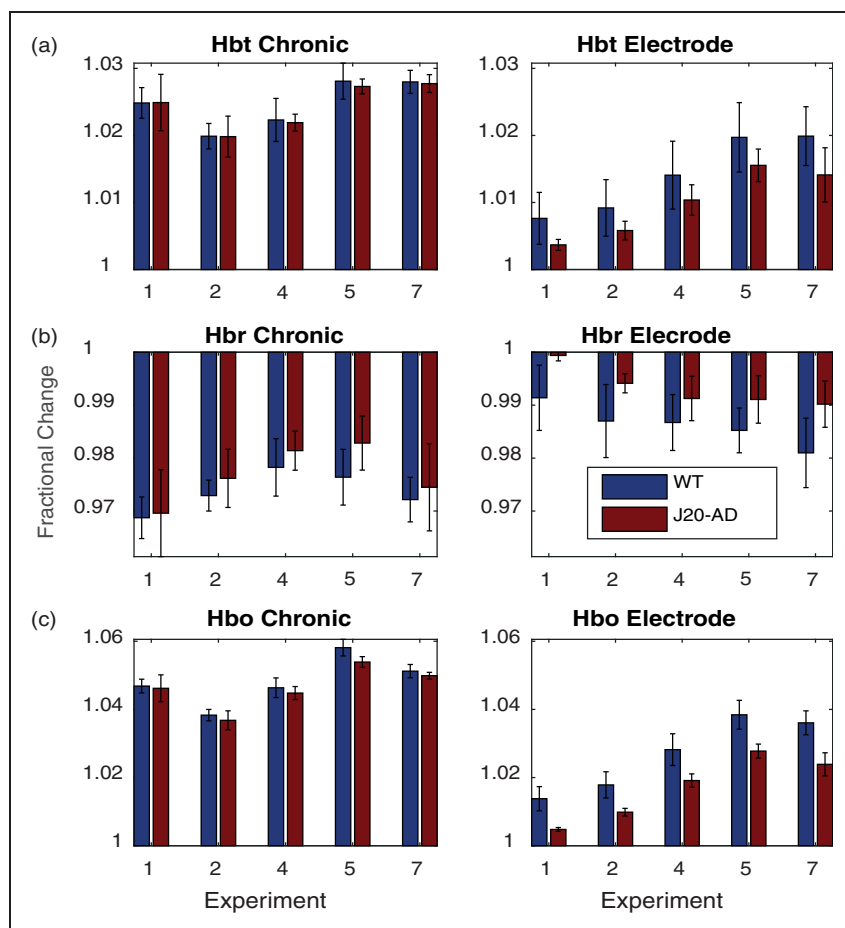


Figure 4. Average magnitude of fractional hemodynamic response for both chronic (left hand side) and acute session (right hand side) stimulation experiments. (a) Hbt (b) Hbr and (c) Hbo. Error bars = standard deviation.

interaction between animal type and session. Thus, for the chronic session with no electrode insertion, there was no overall difference in response between the WT and J20-AD animals. However, for the acute session, significant differences between the groups were observed with the J20-AD responses always lower than the corresponding WT response at the same time point (Figure 4).

Concatenated experimental time course

To better understand the differences between the chronic and acute session results because all our data were collected continuously with small gaps between each of the eight experiments, we were able to concatenate the data for all experiments to produce a longitudinal record of each session in each of the four experimental groups (Figure 5). This figure shows the stability of our chronic anaesthetised protocol (Figure 5(a) and (b)) insofar as, apart from the expected large shifts caused by the gas challenges (Exp3 and Exp6) and hypercapnia (Exp8), the baseline hemodynamic values were remarkably stable.

However, something was clearly different in the acute sessions for both WT (Figure 5(c)) and J20-AD (Figure 5(d)) in which the recording electrode was introduced prior to collecting the imaging data. In these circumstances, the baseline values for both WT and J20-AD seemed to be recovering from a prior event. This was especially evident during the initial phase of the session (exp1 and 2). Also obvious was that the prior event caused the J20-AD perturbation from baseline to be larger than the WT animals. The perturbation at the beginning of the experimental session was indicative of a cortical spreading depression (CSD) that was caused by the acute electrode insertion. We will discuss this further below, after having presented the electrophysiological and hypercapnia data from our study.

Neural responses to stimulation

The field potential responses from the sensory stimulation experiments (Exps 1,2,4,5, and 7) showed remarkably little difference between the WT and AD groups

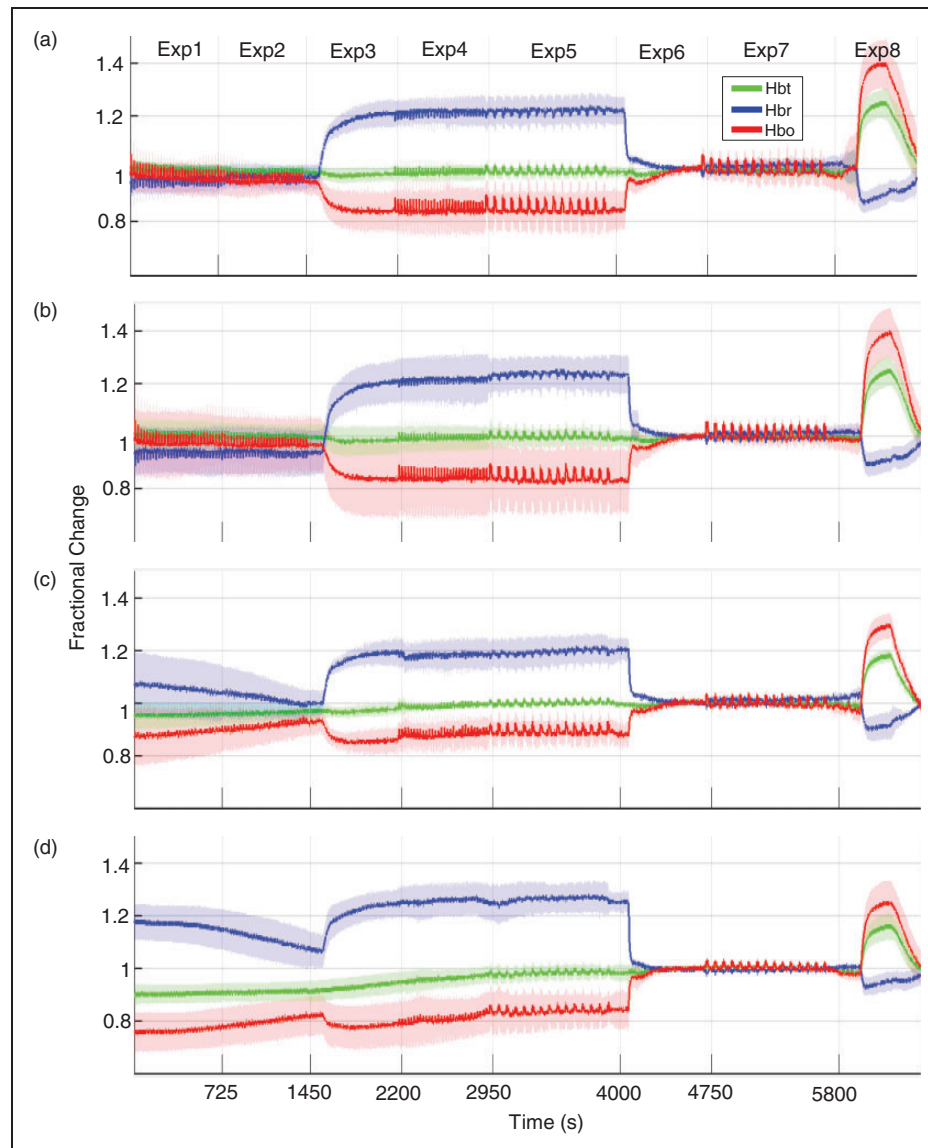


Figure 5. Concatenated hemodynamic times series of responses across experiments for all imaging sessions (a) Wild-type chronic, (b) J20-AD Chronic, (c) Wild-type acute and (d) J20-AD acute. Shaded error bars = standard deviation.

(Figure 6). A repeated measures ANOVA performed on the averaged evoked field potential response recorded from the middle cortical layers (Figure 6, column 4), revealed no reliable differences between the animal type ($F=2.44$, $p=0.13$), experimental condition ($F=1.5$, $p=0.2$) or interaction ($F=1.36$, $p=0.26$). The discrepancy between the acute neural and hemodynamic responses is an important issue and this subject will be discussed further below.

Hypercapnia

To assess the hypercapnia response recorded during the three chronic imaging sessions they were averaged and the mean magnitude of response taken during 250-

500s. T-tests (two tailed distribution, two-sample equal variance) were conducted to test for significant differences between J20-AD and WT. None of the data for Hbt ($p=0.39$), Hbo ($p=0.28$) and Hbr ($p=0.21$) for the two groups were reliably different. There were also no significant differences between the groups in the final acute imaging session (Hbt, $p=0.39$, Hbo, $p=0.23$ and Hbr, $p=0.08$).

Compartmental responses and differences between hemodynamic responses evoked by 2-s sensory stimulation under air and oxygen

As we have collected two-dimensional images over time across all our experimental sessions, principal

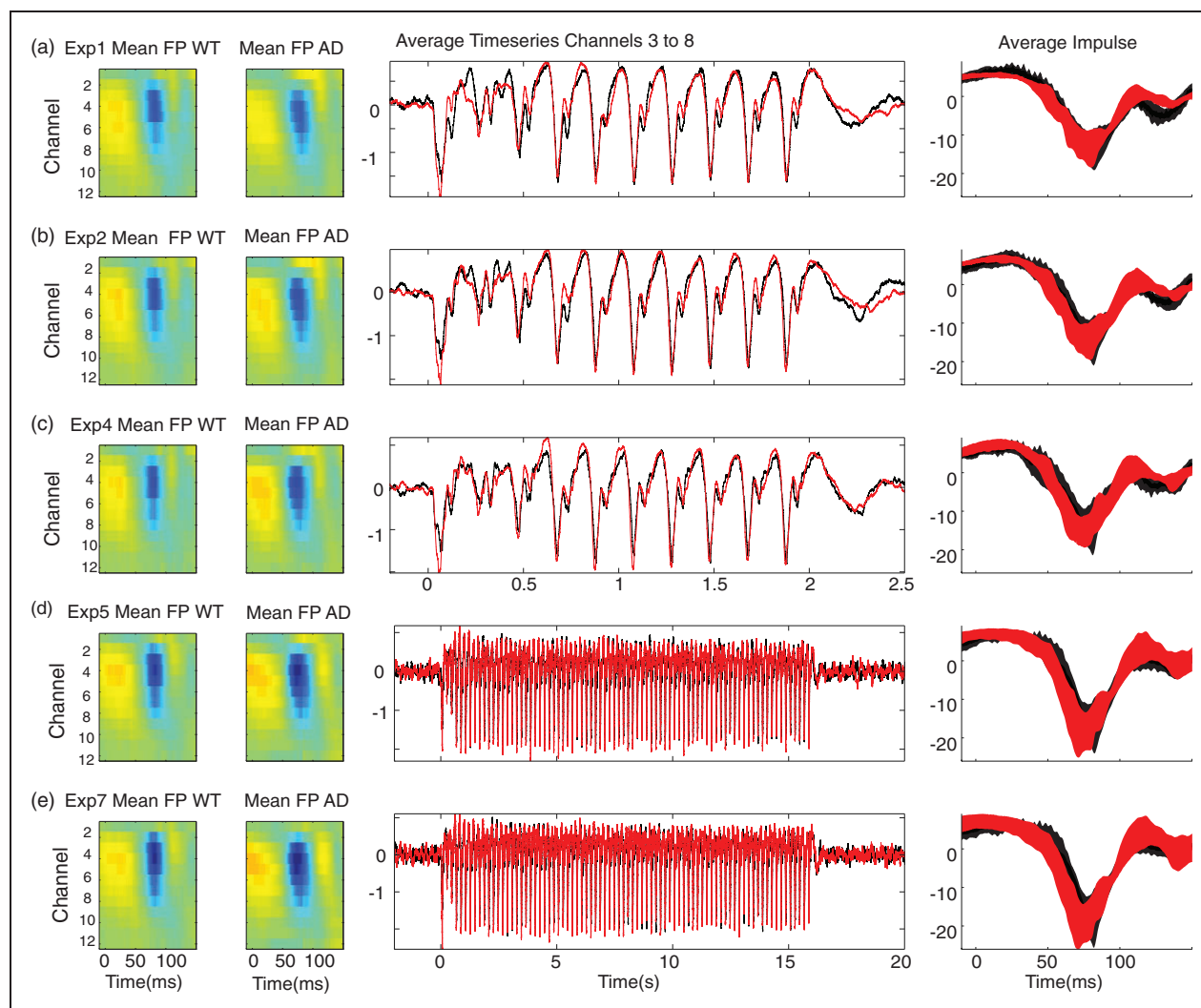


Figure 6. Neural responses from WT and J20-AD mice from stimulation experiments. (a) Exp1, (b) Exp2 (c) Exp4 (d) Exp5 and (e) Exp7. Left hand images represent the averaged single impulse response in the different stimulation experiments. Middle time series represents the average field potential response from channels 3–8 for WT and J20-AD mice. Right hand column represents the averaged time series impulse response from channels 3 to 8. WT = black time series, J20-AD = red time series, Shaded error bars = standard deviation.

component analysis (PCA) was used to extract responses strongly biased towards the surface vessels as they account for most of the variance in the data (Figure 7). For Hbt, the first PCA almost always highlighted major branches of the middle cerebral artery (MCA) responding to the stimulus (Figure 7 (b)). This reflected strong activation of the arterial tree on the surface of the brain. For Hbr, the first PCA showed how strongly the surface veins were changing in saturation as Hbr was decreased due to the large increase in fresh blood arriving to the cortex. After selecting arterial and vein regions (Figure 7(f) to (i)), clear differences were observed in both groups, not only in the magnitude of the chronic and acute responses (described above) but in the return

to baseline depending on whether the animal was breathing 100% oxygen or medical air. Again, in both groups under the air condition, there was a strong post-stimulation undershoot which was largest in the arterial compartment (Figure 7(f)). In the pure oxygen condition, this overshoot was absent again the importance of this observation will be discussed below.

Discussion

Our main finding was that differences between the haemodynamic performance of J20-AD mice and WT controls were dependent on experimental procedure. Under stable conditions of chronic imaging, minimal differences between the J20-AD and WT were observed

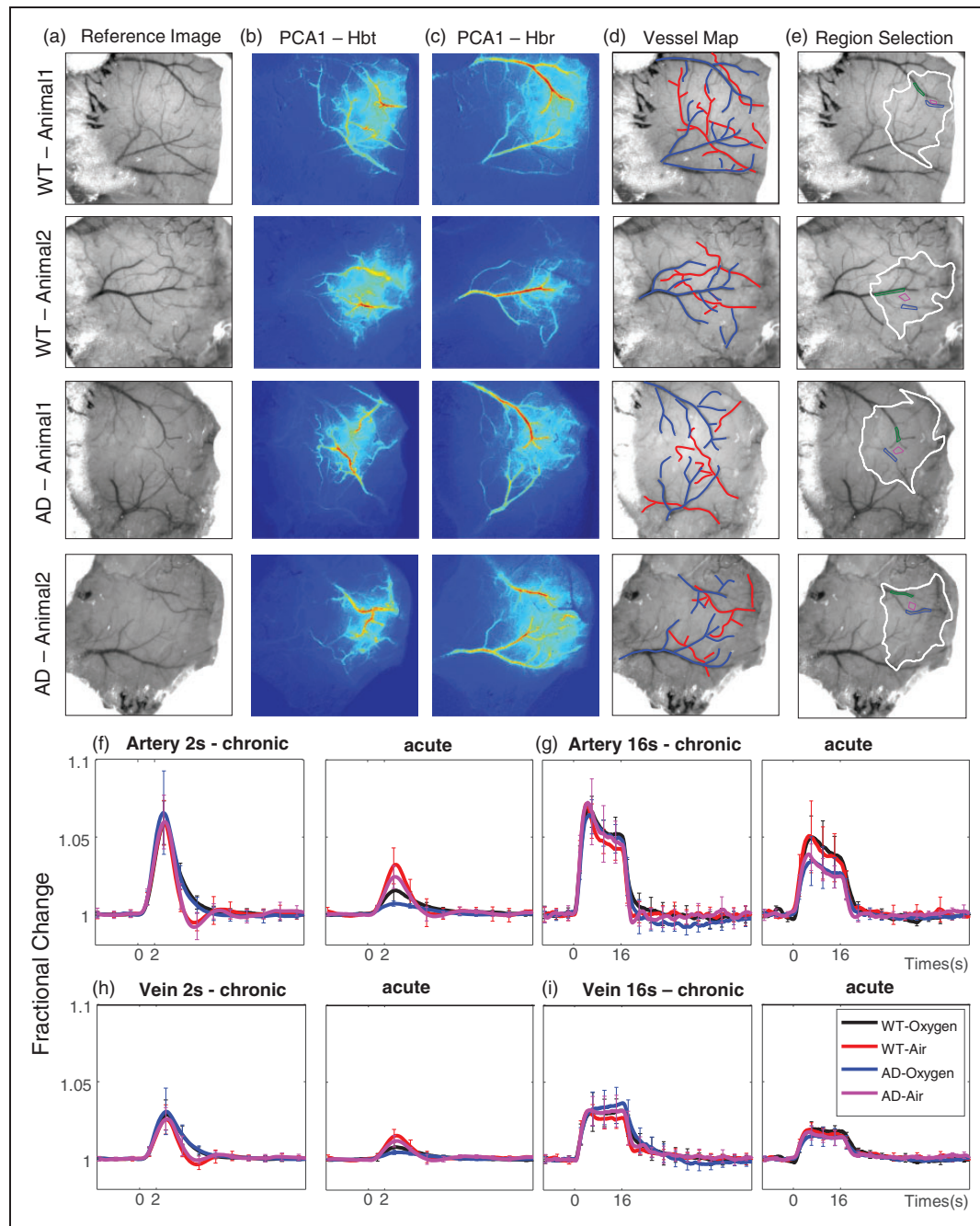


Figure 7. Anatomically compartmentalised vascular responses for four representative animals (a) Reference image showing cortical vasculature (b) The first principal component of the Hbt image data block (c) First principal component of the Hbr image data block. (d) Reference images with superimposed surface arteries (red) and veins (blue) (e) Calculated whisker response region with selected artery and vein regions. (f) Hbt (blood volume) 2-s stimulation response in the arterial compartment for chronic (left) and acute (right) experiments. (g) Hbt 16-s stimulation response in the arterial compartment for chronic (left) and acute (right) experiments. (h) Hbt 2-s stimulation response in the venous compartment for chronic (left) and acute (right) experiments. (i) Hbt 16-s stimulation response in the venous compartment for chronic (left) and acute (right) experiments.

to a wide variety of sensory stimulation and gas challenges. This failed to confirm the previous reports of serious impairments of neurovascular function in the J20-AD model.^{7,8,10} However, in our final experiment, which involved acute experimental procedures, a clear

impairment of haemodynamic responses in the J20-AD animals was observed, similar to previous reports. However, compared to the chronic imaging sessions, we found that the magnitude of evoked-responses of both WT and J20-AD mice was reduced, with the

J20-AD mice affected to a significantly greater extent. We draw a general conclusion that well-controlled procedures are necessary to separate the effects of methodological confounds from genuine effects of pathophysiological changes induced by the disease state being tested.

Preservation of neurovascular coupling in the J20 mouse model of AD

Why in the stable chronic recording phase of our study did we fail to replicate the neurovascular deficits reported previously? First, we used similar whisker stimulation protocols to the studies that reported 35–50% reductions in evoked cerebral blood flow responses of J20-AD mice from seven months of age. Our subjects were 9–12 months old at the start of the study. Both our and previous experiments were all performed with anaesthetised mice. However, previous studies^{7,8,10} conducted few stimulation presentations (4–6 stimulation trials per animal), in the anaesthetised mouse immediately following acute procedures to thin the skull. At the outset, we sought to extend these findings by using 2D-OIS to resolve changes in different vascular compartments with repeated testing in a chronic preparation. Informed by our previous work with an awake head restrained preparation,¹⁴ we adopted a refined anaesthetised protocol that permitted extended (3 h) imaging sessions repeatedly over weeks. Under anaesthesia, the haemodynamic responses evoked by sensory stimulation in this chronic preparation were comparable to those seen previously with awake animals.¹⁴ Another difference was the present protocol involved a more detailed set of experimental variables, i.e. sequences of multiple trials (120) with different duration whisker stimulations (2 s and 16 s), with and without vascular reactivity gas challenges. In addition, our protocol enabled us to generate an average experimental session by averaging the sequence of hemodynamic time series from all chronically prepared subjects (Figure 5). These data show not only that responses to individual sensory stimulations could be observed, but that the haemodynamic baseline values were stable throughout the session. Under our more stringent chronic conditions and more detailed testing, we failed to replicate the previously reported haemodynamic deficits in J20-AD mice. Therefore, our conclusion must be that neurovascular function is still largely preserved in the J20-AD mouse in this age range. This observation also fits with the relatively mild cortical pathology seen in the J20-AD mouse model (Figure 1). Both our group and others^{12,13} have shown the strongest A β plaque deposition at this age point is in the hippocampus, which leads to early deficits in memory and cognitive function. Neurovascular breakdown may be

more prevalent in mouse models with stronger cortical pathology, such as the APP/PS1.¹⁵

Acute experimental conditions

Given these essentially negative results from the first three chronic experimental sessions, we looked for correspondences between haemodynamic and neural responses in a final acute experimental session. Significantly, this phase of the study involved acute experimental conditions akin to those used in the previous investigations.^{7,8,10} After the electrode insertion, we noted that baseline hemodynamics were altered. Specifically, there was a significant reduction in blood volume and saturation that gradually recovered to normal stable levels towards the end of the session. Significantly, the baseline changes were larger for the AD mice compared with the WT controls. We therefore suggest that acute procedures, in our case the insertion of a multi-channel electrode, likely cause a cortical spreading depression (CSD). This is characterised by an alternating vasoconstriction and dilation that can last over 90 min, and is known to affect neurovascular coupling profoundly.^{16,17} Therefore, differential rates of recovery from CSD between the J20-AD and WT mice are the most likely explanation of the differences in haemodynamic performance between the groups.

Furthermore, we present data in an AD animal at the same age (Supplementary Figure 1) where we imaged the electrode being inserted into the cortex prior to performing the same experimental protocols done in this study. The resulting CSD was a direct effect of electrode insertion and produced the typical changes in baseline (described above). This effect is entirely consistent with the baseline changes we saw in the early stages of our acute experiments.

Also importantly, Chang et al.¹⁶ reported that hemodynamic recovery from CSD takes longer than the recovery of neural activity. This could explain the lack of correspondence between the neural (no differences) and haemodynamic measures (significant differences) between the WT and J20-AD groups in the final acute phase of our study. Supporting this interpretation, electrode insertion in mice induced a robust CSD response across the whole cortex.¹⁸ Why should J20 mice be more susceptible to its deleterious effects? It is known that J20 mice exhibit hypertrophic astrocytes and activated microglia in the cortex near beta amyloid plaques.^{12,13} If these cells were sensitized as part of the disease process, the CSD event could be more profound in J20-AD animals. The larger baseline disturbance in the J20-AD animals at the start of recording in the final acute experimental session would be consistent with this suggestion (Figure 5).

Oxygen vs. air response shape

A further unexpected result was that, regardless of mouse model, the shape of hemodynamic response changed according to whether the animal was breathing oxygen or air. The overall response magnitude was reduced and there was an undershoot in the return to baseline when the animals were breathing air, compared with when they were breathing oxygen. This was especially evident following 2-s stimulation, and it was less marked for 16-s stimulation (Figure 7). This difference was driven by the arterial response. In contemporary neurovascular research, the prevailing view is that coupling is more likely to be neurogenic in origin, compared to metabolically driven changes in blood flow.^{19,20} However, as the neural responses evoked by 2-s sensory stimulation were remarkably similar between the air and oxygen conditions (Figure 6), the observed differences appear to be a direct effect of inspired oxygen controlling the arterial response, particularly in the return to baseline. Previous *in vitro* experiments²¹ reported that levels of oxygen could dictate whether an artery dilates or constricts in response to a stimulus, and that this is mediated by different responses of astrocytes. Interestingly, a recent 2-photon microscopy study²² reported similar arterial responses to mouse sensory stimulation. In some cases, the responses had a bi-phasic shape (similar to our air condition) while in others, there was a gradual return to baseline without overshoot (similar to our oxygen condition). No reasons were given to why the same sensory stimulus produced a varying arteriolar response. However, an important conclusion from this aspect of our study is that tissue oxygen levels may be an important determinant of neurovascular control and warrants further investigation.

Limitations of the study

Our current spectroscopy algorithm requires an estimation of both a level of blood volume and saturation. Although, previous published research used LDF, which has a similar weakness, arterial spin labelling studies suggest that baseline CBF is reduced in J20-AD mice.²³ We mitigated these effects by measuring changes in baseline volume and saturation in our animals when switching from breathing oxygen to air. If there were differences in saturation between the two groups, this would be evidence that our estimated baseline values were inaccurate. However, the consistency of the results between the WT and AD mice suggests that under the oxygen condition, our estimates were appropriate. Moreover, even if estimates of volume and saturation were wrong, the fractional change in Hbt response would be unaffected. We have run the

data across a range of assumed Hbt baselines and this produces no difference in the fractional change in Hbt response (Supplementary Figure 2). A final consideration between previous studies using LDF and ours using 2D-OIS is the potential that these methodologies are sampling from different depths of tissue. 2D-OIS measures predominantly from the first 500 μm 's of tissue whereas the LDF can penetrate deeper.²⁴ In future experiments, we will perform LDF simultaneous with 2D-OIS to investigate this possibility.

It must also be noted that all our experiments were performed under light anaesthesia, which of course is a non-physiological state. To some extent, this is mitigated by our previous investigation¹⁴ that showed the responses in the present study were comparable to those seen previously with awake animals. On the positive side, the current anaesthetised preparation provides a more stable imaging platform where the effects of controlled small mechanical stimulations can be observed. Importantly, baseline perturbations, such as caused by the insertion of an electrode, are easier to detect in the absence of uncontrolled motivational and movement variables that are often inherent in awake experimental protocols.

The extent to which the current observations may generalise to other mouse models of AD, and to other time-points during disease progression, remains uncertain. For example, other mouse models at various time points have shown neurovascular deficits (see review by Klohs et al.⁶) including the triple transgenic APPSwDI⁹, Tg2567,²⁵ APP/PS1 and 5FAD mice.²⁶ However, we note that many of these experiments were conducted using acutely anaesthetised preparations. Potentially, this could render them vulnerable to the problem of short-term acute procedures reported in this study. Therefore, the current findings with the J20-AD model should serve as a note of caution that observed deficits could be a result of experimental approach, rather than a measure of disease progression.

Conclusions

Contrary to previous reports of neurovascular deficits J20-AD mice, under the stable chronic imaging conditions, we found that the neurovascular performance of J20-AD did not differ reliably from that of WT controls. However, the acute phase of the current study showed the J20-AD mice to be more susceptible to disruptive interventions, such as the acute experimental procedures used in the current study. The J20-AD mouse model may, therefore, represent an ideal model to explore the effects of mixed pathologies with conditions such as atherosclerosis that would further compromise neurovascular function.

Funding

The author(s) disclosed receipt of the following financial support for the research, authorship, and/or publication of this article: This work was supported by Alzheimer's Research UK (grant number ARUK-IRG2014) and the Medical Research Council UK (grant number MR/M013553/1). Clare Howarth is funded by a Sir Henry Dale Fellowship jointly funded by the Wellcome Trust and the Royal Society (Grant Number 105586/Z/14/Z).

Acknowledgements

We thank Dr. Lennart Mucke (Gladstone Institute of Neurological Disease and Department of Neurology, UCSF, CA) and the J. David Gladstone Institutes for the hAPPSwe, Ind mice. The authors would also like to thank Michael Port for his technical assistance.

Declaration of conflicting interests

The author(s) declared no potential conflicts of interest with respect to the research, authorship, and/or publication of this article.


Authors' contributions

All authors proofread and edited the manuscript, PS designed and carried out the study, KA performed histology, LB designed and built the imaging apparatus, SH performed statistical analysis, CH performed data analysis, OS performed data analysis, SW advised on experimental design. PR advised on data analysis and final drafting of the manuscript. JB conceived the study, performed data analysis and wrote the manuscript.

ORCID iDs

Kamar E Ameen-Ali  <https://orcid.org/0000-0002-7583-4099>

Luke Boorman  <https://orcid.org/0000-0001-5189-0232>

Clare Howarth  <https://orcid.org/0000-0002-6660-9770>

Supplemental material

Supplemental material for this article is available online.

References

- Hardy J. An 'anatomical cascade hypothesis' for Alzheimer's disease. *Trends Neurosci* 1992; 15: 200–201.
- Zlokovic BV. Neurodegeneration and the neurovascular unit. *Nat Med* 2010; 16: 1370–1371.
- Zlokovic BV. Neurovascular pathways to neurodegeneration in Alzheimer's disease and other disorders. *Nat Rev Neurosci* 2011; 12: 723–738.
- Iturria-Medina Y, Sotero RC, Toussaint PJ, et al. Early role of vascular dysregulation on late-onset Alzheimer's disease based on multifactorial data-driven analysis. *Nat Commun* 2016; 7: 11934.
- Ameen-Ali KE, Wharton SB, Simpson JE, et al. Review: neuropathology and behavioural features of transgenic murine models of Alzheimer's disease. *Neuropathol Appl Neurobiol* 2017; 43: 553–570.
- Klohs J, Rudin M, Shimshek DR, et al. Imaging of cerebrovascular pathology in animal models of Alzheimer's disease. *Front Aging Neurosci* 2014; 6: 32.
- Lacoste B, Tong XK, Lahjouji K, et al. Cognitive and cerebrovascular improvements following kinin B1 receptor blockade in Alzheimer's disease mice. *J Neuroinflammation* 2013; 10: 57.
- Ongali B, Nicolakakis N, Tong XK, et al. Angiotensin II type 1 receptor blocker losartan prevents and rescues cerebrovascular, neuropathological and cognitive deficits in an Alzheimer's disease model. *Neurobiol Dis* 2014; 68: 126–136.
- Park L, Koizumi K, El Jamal S, et al. Age-dependent neurovascular dysfunction and damage in a mouse model of cerebral amyloid angiopathy. *Stroke* 2014; 45: 1815–1821.
- Royea J, Zhang L, Tong XK, et al. Angiotensin IV receptors mediate the cognitive and cerebrovascular benefits of losartan in a mouse model of Alzheimer's disease. *J Neurosci* 2017; 37: 5562–5573.
- Tarantini S, Fulop GA, Kiss T, et al. Demonstration of impaired neurovascular coupling responses in TG2576 mouse model of Alzheimer's disease using functional laser speckle contrast imaging. *Geroscience* 2017; 39: 465–473.
- Ameen-Ali KE, Simpson JE, Wharton SB, et al. The time course of recognition memory impairment and glial pathology in the hAPP-J20 mouse model of Alzheimer's disease. *J Alzheimers Dis* 2019; 68: 609–624.
- Wright AL, Zinn R, Hohensinn B, et al. Neuroinflammation and neuronal loss precede Abeta plaque deposition in the hAPP-J20 mouse model of Alzheimer's disease. *PLoS One* 2013; 8: e59586.
- Sharp PS, Shaw K, Boorman L, et al. Comparison of stimulus-evoked cerebral hemodynamics in the awake mouse and under a novel anesthetic regime. *Sci Rep* 2015; 5: 12621.
- Reyes-Marin KE and Nunez A. Seizure susceptibility in the APP/PS1 mouse model of Alzheimer's disease and relationship with amyloid beta plaques. *Brain Res* 2017; 1677: 93–100.
- Chang JC, Shook LL, Biag J, et al. Biphasic direct current shift, haemoglobin desaturation and neurovascular uncoupling in cortical spreading depression. *Brain* 2010; 133: 996–1012.
- Piilgaard H and Lauritzen M. Persistent increase in oxygen consumption and impaired neurovascular coupling after spreading depression in rat neocortex. *J Cereb Blood Flow Metab* 2009; 29: 1517–1527.
- Eles JR, Vazquez AL, Kozai TDY, et al. In vivo imaging of neuronal calcium during electrode implantation: spatial and temporal mapping of damage and recovery. *Biomaterials* 2018; 174: 79–94.
- Kennerley AJ, Harris S, Bruyns-Haylett M, et al. Early and late stimulus-evoked cortical hemodynamic responses provide insight into the neurogenic nature of neurovascular coupling. *J Cereb Blood Flow Metab* 2012; 32: 468–480.

20. Urban A, Rancillac A, Martinez L, et al. Deciphering the neuronal circuitry controlling local blood flow in the cerebral cortex with optogenetics in PV::Cre transgenic mice. *Front Pharmacol* 2012; 3: 105.
21. Gordon GR, Choi HB, Rungta RL, et al. Brain metabolism dictates the polarity of astrocyte control over arterioles. *Nature* 2008; 456: 745–749.
22. Uhlirova H, Kilic K, Tian P, et al. Cell type specificity of neurovascular coupling in cerebral cortex. *eLife* 2016; 5: e14315.
23. Hebert F, Grand'maison M, Ho MK, et al. Cortical atrophy and hypoperfusion in a transgenic mouse model of Alzheimer's disease. *Neurobiol Aging* 2013; 34: 1644–1652.
24. Berwick J, Johnston D, Jones M, et al. Neurovascular coupling investigated with two-dimensional optical imaging spectroscopy in rat whisker barrel cortex. *Eur J Neurosci* 2005; 22: 1655–1666.
25. Han BH, Zhou ML, Abousaleh F, et al. Cerebrovascular dysfunction in amyloid precursor protein transgenic mice: contribution of soluble and insoluble amyloid-beta peptide, partial restoration via gamma-secretase inhibition. *J Neurosci* 2008; 28: 13542–13550.
26. Cruz Hernandez JC, Bracko O, Kersbergen CJ, et al. Neutrophil adhesion in brain capillaries reduces cortical blood flow and impairs memory function in Alzheimer's disease mouse models. *Nat Neurosci* 2019; 22: 413–420.